

Where angular momentum goes in a precessing black hole binary

Carlos O. Lousto and Yosef Zlochower

Center for Computational Relativity and Gravitation,
School of Mathematical Sciences, Rochester Institute of Technology,
85 Lomb Memorial Drive, Rochester, New York 14623
(Dated: August 3, 2018)

We evolve a set of 32 equal-mass black-hole binaries with collinear spins (with intrinsic spin magnitudes $|\vec{S}_{1,2}/m_{1,2}^2| = 0.8$) to study the effects of precession in the highly nonlinear plunge and merger regimes. We compare the direction of the instantaneous radiated angular momentum, $\delta\vec{J}_{\text{rad}}(t)$, to the directions of the total angular momentum, $\vec{J}(t)$, and the orbital angular momentum, $\vec{L}(t)$. We find that $\delta\vec{J}_{\text{rad}}(t)$ approximately follows \vec{L} throughout the evolution. During the orbital evolution and merger, we observe that the angle between \vec{L} and total spin \vec{S} is approximately conserved to within 1° , which allows us to propose and test models for the merger remnant's mass and spin. For instance, we verify that the *hangup* effect is the dominant effect and largely explains the observed total energy and angular momentum radiated by these precessing systems. We also verify that the total angular momentum, which significantly decreases in magnitude during the inspiral, varies in direction by less than $\sim 5^\circ$. The maximum variation in the direction of \vec{J} occurs when the spins are nearly antialigned with the orbital angular momentum. Based on our results, we conjecture that transitional precession, which would lead to large variations in the direction of \vec{J} , is not possible for similar-mass binaries and would require a mass ratio $m_1/m_2 \lesssim 1/4$.

PACS numbers: 04.25.dg, 04.25.Nx, 04.30.Db, 04.70.Bw

INTRODUCTION AND MOTIVATION

The 2005 breakthroughs in Numerical Relativity [1–3] allowed for accurate investigations of the orbital motion of merging black-hole binaries (BHBs) in the highly-nonlinear regime between the slow inspiral (which can be modeled by post-Newtonian dynamics) and the post-merger phase (which can be modeled by black-hole perturbation theory). In particular it allowed numerical relativists to quantify the effects of black-hole spin in the last stages of the merger. This includes notable effects such as the *hangup* effect [4], which delays or expedites the merger depending on whether the spins are aligned or counter-aligned with the orbital angular momentum, and the generation of recoils as large as several thousand km s^{-1} when the spins are (at least partially) antialigned with each other and have a nontrivial components in the orbital plane [5, 6].

Here we investigate the effects of precession of the BHB system on the evolution of the total angular momentum, \vec{J} , the orbital angular momentum, \vec{L} , the total spin, \vec{S} , and the instantaneous radiated angular momentum $\delta\vec{J}_{\text{rad}} = -d\vec{J}/dt$, during the plunge and merger of the binary, a regime that cannot be accurately modeled within the post-Newtonian framework.

Radiation of energy and angular momentum causes the orbit of a binary to decay, leading to an eventual merger. If the energy is radiated preferentially in one direction, the remnant will recoil. Similarly, determining how much of, and in which directions, the angular momentum is radiated allows us to accurately model the remnant's spin.

This is important, for instance, in modeling the evolution of black-hole spins by successive mergers in models of structure growth in the early (high- z) universe [7, 8] as well as for modeling gravitational waveforms for source identification [9–11] and for predicting observational consequences in circumbinary disks [12].

Intimately related to the question of what is the dominant contribution to the final spin of merging black holes is the question of whether *transitional* precession is possible for equal mass (or other mass ratios) black holes in the strong field regime of the plunge and merger. Transitional precession occurs when a binary system transitions from a regime where \vec{J} is dominated by \vec{L} to one where \vec{S} dominates before the merger, passing through a regime where $\vec{L} \approx -\vec{S}$ and \vec{J} can undergo dramatic “flips” in direction [13]. The complementary regime where \vec{L} dominates is called *simple* precession and radiation of angular momentum takes place along $\vec{L} \approx \vec{J}$, which leaves the \vec{J} direction almost unchanged, although its magnitude decreases steadily.

NUMERICAL SIMULATIONS

To single out precession effects, we choose configurations that have equal-mass and equal-spin (magnitude and direction) BHs. These configurations [14] are symmetric under parity [i.e. $(x, y, z) \rightarrow (-x, -y, -z)$] and, consequently, there is no recoil of the final remnant. Such configurations maximize $|\vec{S}| = |\vec{S}_1 + \vec{S}_2|$ and hence the precession in the equal-mass case, which can be seen from

Eq. (2.23a) of Ref. [15],

$$\frac{d\vec{S}}{dt} = \frac{7}{2r^3}(\vec{L} \times \vec{S}) + \frac{3}{r^3}(\hat{n} \cdot \vec{S})(\hat{n} \times \vec{S}), \quad [\vec{n} = \vec{r}_1 - \vec{r}_2]. \quad (1)$$

We also see from Eq. (3.28c) of Ref. [16], that the equal-mass-aligned-spins configuration maximizes the spin-orbit contribution to the radiation of total angular momentum perpendicular to \vec{J} itself.

We vary the polar and azimuthal directions of the initial spins (θ, ϕ) with respect to \hat{L} in order to “cover” the sphere with 32 simulations to find the specific configurations that maximize either precession or the evolution of the direction of $\vec{J}(t)$. The family of BHBs considered here are equal-mass, equal-spins, $|\vec{S}_{1,2}/m_{1,2}^2| = 0.8$, BHBs that are further characterized by three parameters, the initial orbital frequency, the polar inclination of the individual BH spins, and the azimuthal orientation of the spins. For each polar angle θ we evolve a set of six azimuthal angles $\phi = 0^\circ, 30^\circ, \dots, 150^\circ$ (except for $\theta = 0^\circ$ and $\theta = 180^\circ$). We choose initial polar angles equidistant in $\cos \theta$, $\theta = 0^\circ, 48.2^\circ, 70.5^\circ, 90^\circ, 109.5^\circ, 131.8^\circ, 180^\circ$. We start from large enough initial separations to ensure 4 to 6 orbits prior to the merger.

Our numerical evolutions are based on the LAZEV [17] implementation of the moving puncture approach [2, 3] with the conformal function W [18]. Our code uses the CACTUS/EINSTEINTOOLKIT [19, 20] infrastructure and the CARPET [21] mesh refinement driver. We use the TWO PUNCTURES thorn [22] to generate initial data and use the AHFINDERDIRECT code [23] to locate apparent horizons. We measure the horizon mass and spin using the isolated horizon (IH) algorithm of [24]. We use the “flux-linkages” formalism [25], written in terms of ψ_4 [26, 27], to calculate the radiated angular momentum $\delta\vec{J}_{\text{rad}}$.

We define the total angular momentum at time t as $\vec{J}(t) = \vec{J}_{\text{ADM}} - \int_0^t \delta\vec{J}_{\text{rad}}(\tau) d\tau$, which measures the angular momentum on the slice up to the extraction radius (here $R = 100M$). We then translate the radiative quantities in time by R , which is an accurate enough measure of the propagation time for our current purposes.

We used two different techniques to measure the direction of the orbital angular momentum. First, we use the coordinate trajectory $\vec{r}(t)$ and compute $\hat{L}_{\text{coord}} \propto \vec{r}(t) \times \dot{\vec{r}}(t)$; second, we use $\vec{L}(t) = \vec{J}(t) - \vec{S}(t)$, where $\vec{S}(t)$ is measured using the IH algorithm (its direction is inferred from the zeros of the approximate Killing field [14]). We use this second definition in our computations although we verified that our statements below are in agreement with both definitions. We also verified [28] that they both follow the general directions of Refs. [9, 11, 29], which define radiation-based measures of preferred (noninertial) asymptotic frames (see also Fig. 1).

TABLE I: The change in the direction and magnitude of \vec{J} for different θ configurations. Here $\{\vec{A}, \vec{B}\} = \cos^{-1}(\hat{A} \cdot \hat{B})$ measures the angle between two vectors and $\Delta J = |\vec{J}(\infty) - \vec{J}(0)|$ is the magnitude of the net change in \vec{J} over the entire simulation.

$\cos \theta$	2/3	1/3	0	-1/3	-2/3
$\max_{t\phi} \{\hat{J}(t), \hat{J}(0)\}$	0.86°	1.42°	2.33°	3.00°	4.33°
$\max_{t\phi} \{\delta\hat{J}(t), \hat{J}(t)\}$	15.68°	21.53°	25.18°	27.39°	27.12°
$ \vec{J}_{\text{final}} /M_{\text{ADM}}^2$	0.778	0.757	0.725	0.651	0.555
$\Delta J/J_{\text{init}}$	0.352	0.321	0.290	0.311	0.332

RESULTS

In Fig. 1 we show the results from a prototypical simulation. We plot the trajectories of \hat{J} , \hat{L} , \hat{S} , and $\delta\hat{J}_{\text{rad}}$. Note how \hat{J} is nearly constant (an important feature for modeling), the large precession of \hat{L} and \hat{S} , and that the instantaneous direction of the radiated angular momentum is close to \hat{L} .

We denote the angle between two vectors using $\{\vec{A}, \vec{B}\} = \cos^{-1}(\hat{A} \cdot \hat{B})$. While \vec{J} changes in magnitude by more than 30%, the direction of \vec{J} is largely unchanged during the entire simulation (a result also observed in [30]). We thus only observe *simple* precession in these equal-mass BHBs. As seen in Table I and Fig 2, the net motion of \hat{J} (i.e. $\{\vec{J}(t), \vec{J}(0)\}$) is under 5°. The table also shows how far $\delta\vec{J}_{\text{rad}}(t)$ deviates from \hat{J} ($\{\delta\vec{J}_{\text{rad}}(t), \vec{J}(0)\}$) for selected runs.

In Fig. 3 we show the time dependence of the angles $\{\vec{S}(t), \vec{J}(t)\}$, $\{\vec{L}(t), \vec{J}(t)\}$, and $\{\vec{S}(t), \vec{L}(t)\}$. Compared to the precession of $\vec{J}(t)$, the angles between $\vec{J}(t)$ and $\vec{S}(t)$ and $\vec{J}(t)$ and $\vec{L}(t)$ vary more strongly, changing by up to 7° during the inspiral/plunge. From very large separations, when $\vec{J}(t)$ is dominated by $\vec{L}(t)$, the angle between these two vectors secularly increases due to the radiative loss of angular momentum. Consequently, the angle between $\vec{J}(t)$ and $\vec{S}(t)$ decreases to keep the angle between \vec{L} and \vec{S} , nearly constant (with oscillations of $\lesssim 1^\circ$ that can be associated with conservative post-Newtonian dynamics, i.e., nutation). This latter result is very important and will be used in the development of an empirical formula for the final remnant mass and spin since it connects the binary’s configuration at large separations with that at merger [28].

Here we propose a simple model of the final remnant BH’s intrinsic spin and mass based on the observations that the total spin magnitude is conserved to a very high degree during the simulation and that the direction between the instantaneous orbital angular momentum and the total spin is approximately conserved (see also [30]). Given the assumption that, even for precessing binaries, the component of the total spin along the orbital angular momentum leads to the well-known *hangup* effect [4], we

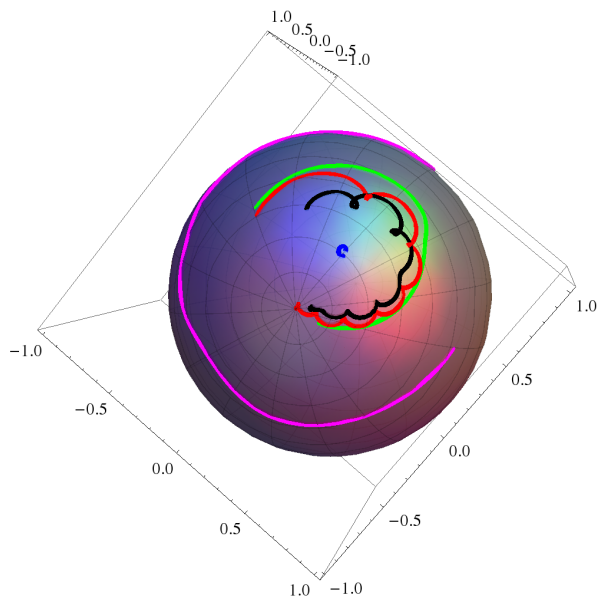


FIG. 1: A plot comparing the trajectories of (successively outwards curves) \hat{J} (small blue curve), $\delta\hat{J}_{\text{rad}}$ (black curve), the coordinate \hat{L} (red curve), \hat{L} as defined by $\hat{L} = \hat{J} - \hat{S}$ (green curve), and $\hat{S}_1 = \hat{S}_2$ (magenta curve) for a $\theta = 90^\circ$ configuration. All vectors move counterclockwise with time.

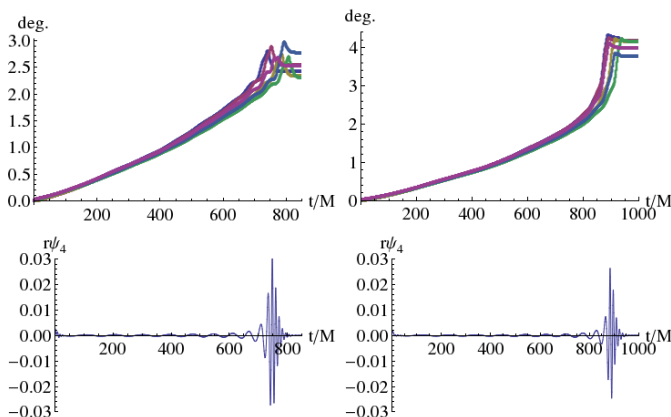


FIG. 2: The precession of \hat{J} (compared to its initial direction) as a function of time for all the $\theta = 110^\circ$ and $\theta = 132^\circ$ configurations (left and right, respectively). The bottom plots show the $(\ell = 2, m = 2)$ mode of ψ_4 with the same time scale as a reference. Note that the precession angle decreases slightly after the large burst of radiation at merger. All 32 cases studied exhibit *simple* precession.

find that the remnant final spin is given by the *hangup* spin with the addition of the in-plane component of the initial total spin. That is, the remnant specific spin magnitude is given by

$$\alpha_{\text{rem}} = \sqrt{F \left(\frac{S_{\parallel}}{2m_h^2} \right)^2 + S_{\perp}^2/M_h^2}, \quad (2)$$

where $F(\alpha)$ is the predicted final remnant spin for the

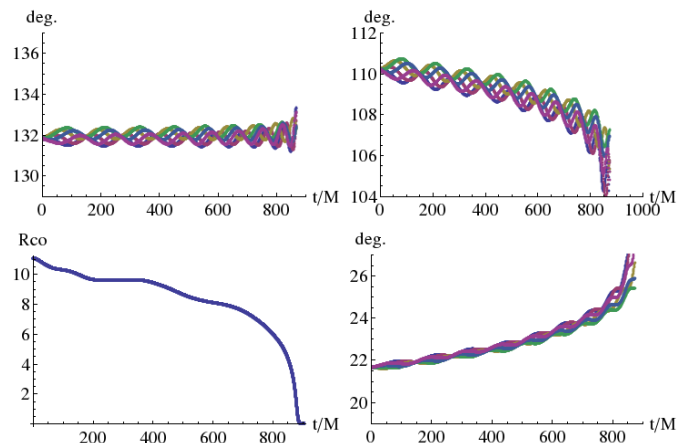


FIG. 3: On the left, the upper plot shows the angle between \hat{L} and $\hat{S}_1 = \hat{S}_2$ for all the $\theta = 132^\circ$ configurations and the bottom plot shows the orbital separation versus time for reference. On the right, the upper plot shows the angle between \hat{J} and $\hat{S}_1 = \hat{S}_2$ and the bottom plot shows the angle between \hat{J} and \hat{L} .

hangup configuration (an equal-mass, equal-spin, non-precessing configuration where both BH spins are aligned with the orbital angular momentum and have intrinsic magnitude α), S_{\parallel} is the component of the total spin in the direction of the orbital angular momentum of the individual BH spin (the factor of 1/2 comes from the fact that $\vec{S} = 2\vec{S}_1 = 2\vec{S}_2$ here), S_{\perp} is the magnitude of the total spin in the orbital plane, m_h is the horizon mass of the individual BHs, and M_h is the mass of the final remnant. To evaluate $F(\alpha)$ we use the recent work of Hemberger *et al.* [31]. We also model the total radiated energy relative to the mass of the BHB when it was infinitely separated, i.e. $\delta\tilde{e} = (2m_h - M_h)/(2m_h)$. Here we measure M_h directly using the IH formalism (denoted by $\delta\tilde{e}_{\text{IH}}$), and by using the relation $M_h = M_{\text{ADM}} - E_{\text{rad}}$ (denoted by $\delta\tilde{e}_{\text{rad}}$). As shown in Fig. 4, we find very good agreement between Eq. (2) and the measured final spins for all configurations studied here. We also find good qualitative agreement between the *hangup* prediction for the radiated energy and our results. However, an excess of radiated energy is apparent due to further nonlinear dependence on the perpendicular component of the spins to be modeled in [28].

DISCUSSION

We performed a set of numerical simulations to explore the effects of precession in the fully nonlinear regime. We chose a simple configuration with equal-mass BHs to complement particle limit studies, and we chose (relatively) large, collinear spins to maximize the precession effects. We found that in this highly nonlinear regime the angles between \vec{J} and \vec{S} or \vec{L} exhibit significant changes

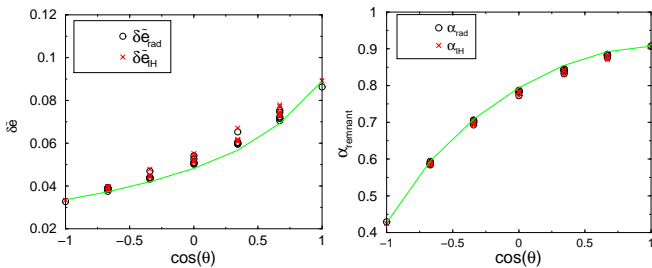


FIG. 4: Radiated energy and remnant specific spin, as calculated using the Isolated Horizon formalism and from the radiated energy-momentum for the 32 simulations, as well as the theoretical predictions for these remnant parameters based on the formulas for the *hangup* remnant from [31]. The different points at the same polar angle correspond to different azimuthal angles, $\phi = 0^\circ - 150^\circ$. No curve fitting was performed in these plots.

on secular time scales with smaller oscillatory changes on the orbital time scale (nutations). On the other hand, the angle between \vec{S} and \vec{L} only shows small oscillations on the orbital time scale with no large secular trend. While the latter was first observed using low-order post-Newtonian theory [13], we see that, perhaps unexpectedly, it continues to hold true in the highly-nonlinear merger regime. We also compute the variation of the direction of the total angular momentum of the system as seen far from the sources and find that it varies at most by $\sim 5^\circ$ for our runs and hence is limited by $\sim 7^\circ$ for even maximally spinning holes. These results, connecting early and late time binary dynamics, are very important for modeling the remnant final masses and spins of the merged black hole with applications to cosmological and astrophysical scenarios, and for gravitational wave modeling. We verified that these assumptions work well when we compared the total energy radiated and final spins of our simulation with those of the *hangup* configurations, derived for nonprecessing binaries.

The approximate conservation of the total angular momentum direction $\hat{J}(t)$ raises the question of where the radiated angular momentum of the system goes. At large separations, $\vec{J}(t)$ and \vec{L} are almost aligned with each other, but at the closer separations that we study here this needs not to be the case. As shown in Fig. 1, the radiated angular momentum roughly follows the instantaneous direction of the orbital angular momentum $\vec{L}(t)$ rather than the more constant $\vec{J}(t)$. Notably, even though a large amount of angular momentum is radiated over time, this has a relatively small impact on the final direction of \vec{J} , which is a consequence of the fact that $\vec{L}(t)$ itself precesses roughly around \vec{J} , which effectively cancels the net components of $\delta \vec{J}_{\text{rad}}$ perpendicular to $\vec{J}(t)$.

Our configurations with equal mass binaries only exhibit *simple* precession; i.e. the direction of $\vec{J}(t)$ does not

change significantly from its initial direction. When one considers unequal mass binaries, it is possible to fine-tune the parameters of the system so that \vec{J} changes dramatically. To estimate at which mass ratio q this *transitional* precession [13] may occur, we consider the particle limit case of antialigned, maximally spinning holes with the (minimal) orbital angular momentum (at the ISCO [32]). Then for $q = m_1/m_2$, $S_1 = m_1^2$, $S_2 = m_2^2$ we have

$$-L_{\text{ISCO}}^z = \frac{22}{3\sqrt{3}} \frac{q}{(1+q)^2} m^2 \approx S^z = \frac{(1+q^2)}{(1+q)^2} m^2, \quad (3)$$

which leads to a critical $q_c \approx 1/4$, above which transitional precession is not possible.

The relevance of including the spin dependence in the waveforms of coalescing black hole binaries to improve the sensitivity of a search, even in the nonprecessing case, was recently quantified in Ref. [33]. Precession effects will further modulate the waveform. Recently, a new method [9–11, 34] for generating precessing waveforms by rotating nonprecessing (*hangup*) waveforms was developed. Our work lends support to this method since we observe that the binary dynamics are dominated by the nonprecessing *hangup* effect. This is a consequence of the conservation of the angle between \vec{L} and \vec{S} . Note that this *hangup* waveform will have to be modified during the latest stages of merger to account for the true total spin as in Eq. (2) (e.g., to get the correct ringdown frequency). Similarly, an accurate prediction of the final mass and spin of the merged black hole is crucial for phenomenological descriptions of the gravitational waveforms, such as those based on SEOBNR [35].

In addition, the relevance of these results for astrophysical scenarios lies on the fact that gravitational radiation, even for highly precessing systems, hardly changes the direction of the total angular momentum of the system. Thus suggesting [30], for instance, that AGN jets, which are associated with the direction of the spin of the central black hole engine, are good indicators of the direction of the total angular momentum of the progenitor binary system. While the accurate modeling of the remnant mass leads to specific predictions for the spectrum of the cosmological gravitational-waves background radiation that could discern between light and heavy seeds scenarios [36].

The authors gratefully acknowledge the NSF for financial support from Grants PHY-1305730, PHY-1212426, PHY-1229173, AST-1028087, PHY-0969855, OCI-0832606, and DRL-1136221. Computational resources were provided by XSEDE allocation TG-PHY060027N, and by NewHorizons and BlueSky Clusters at Rochester Institute of Technology, which were supported by NSF grant No. PHY-0722703, DMS-0820923, AST-1028087, and PHY-1229173.

-
- [1] F. Pretorius, Phys. Rev. Lett. **95**, 121101 (2005), gr-qc/0507014.
- [2] M. Campanelli, C. O. Lousto, P. Marronetti, and Y. Zlochower, Phys. Rev. Lett. **96**, 111101 (2006), gr-qc/0511048.
- [3] J. G. Baker, J. Centrella, D.-I. Choi, M. Koppitz, and J. van Meter, Phys. Rev. Lett. **96**, 111102 (2006), gr-qc/0511103.
- [4] M. Campanelli, C. O. Lousto, and Y. Zlochower, Phys. Rev. **D74**, 041501(R) (2006), gr-qc/0604012.
- [5] M. Campanelli, C. O. Lousto, Y. Zlochower, and D. Merritt, Phys. Rev. Lett. **98**, 231102 (2007), gr-qc/0702133.
- [6] C. O. Lousto and Y. Zlochower, Phys. Rev. Lett. **107**, 231102 (2011), 1108.2009.
- [7] M. Volonteri, M. Sikora, J.-P. Lasota, and A. Merloni (2012), 1210.1025.
- [8] P. Amaro-Seoane, S. Konstantinidis, M. D. Freitag, M. C. Miller, and F. A. Rasio (2012), 1211.6738.
- [9] P. Schmidt, M. Hannam, and S. Husa, Phys. Rev. **D86**, 104063 (2012), 1207.3088.
- [10] L. Pekowsky, R. O’Shaughnessy, J. Healy, and D. Shoemaker (2013), 1304.3176.
- [11] M. Boyle (2013), 1302.2919.
- [12] S. C. Noble, B. C. Mundim, H. Nakano, J. H. Krolik, M. Campanelli, Y. Zlochower, and N. Yunes, Astrophys. J. **755**, 51 (2012), 1204.1073.
- [13] T. A. Apostolatos, C. Cutler, G. J. Sussman, and K. S. Thorne, Phys. Rev. D **49**, 6274 (1994).
- [14] M. Campanelli, C. O. Lousto, Y. Zlochower, B. Krishnan, and D. Merritt, Phys. Rev. **D75**, 064030 (2007), gr-qc/0612076.
- [15] E. Racine, A. Buonanno, and L. E. Kidder, Phys. Rev. **D80**, 044010 (2009), 0812.4413.
- [16] L. E. Kidder, Phys. Rev. **D52**, 821 (1995), gr-qc/9506022.
- [17] Y. Zlochower, J. G. Baker, M. Campanelli, and C. O. Lousto, Phys. Rev. **D72**, 024021 (2005), gr-qc/0505055.
- [18] P. Marronetti, W. Tichy, B. Brügmann, J. Gonzalez, and U. Sperhake, Phys. Rev. **D77**, 064010 (2008), 0709.2160.
- [19] Cactus Computational Toolkit home page: <http://cactuscode.org>.
- [20] Einstein Toolkit home page: <http://einstein toolkit.org>.
- [21] E. Schnetter, S. H. Hawley, and I. Hawke, Class. Quant. Grav. **21**, 1465 (2004), gr-qc/0310042.
- [22] M. Ansorg, B. Brügmann, and W. Tichy, Phys. Rev. **D70**, 064011 (2004), gr-qc/0404056.
- [23] J. Thornburg, Class. Quant. Grav. **21**, 743 (2004), gr-qc/0306056.
- [24] O. Dreyer, B. Krishnan, D. Shoemaker, and E. Schnetter, Phys. Rev. **D67**, 024018 (2003), gr-qc/0206008.
- [25] J. Winicour, in *General Relativity and Gravitation Vol 2*, edited by A. Held (Plenum, New York, 1980), pp. 71–96.
- [26] M. Campanelli and C. O. Lousto, Phys. Rev. **D59**, 124022 (1999), gr-qc/9811019.
- [27] C. O. Lousto and Y. Zlochower, Phys. Rev. **D76**, 041502(R) (2007), gr-qc/0703061.
- [28] C. O. Lousto and Y. Zlochower (2013), 1312.5775.
- [29] R. O’Shaughnessy, J. Healy, L. London, Z. Meeks, and D. Shoemaker, Phys. Rev. **D85**, 084003 (2012), 1201.2113.
- [30] E. Barausse and L. Rezzolla, Astrophys. J. Lett. **704**, L40 (2009), 0904.2577.
- [31] D. A. Hemberger, G. Lovelace, T. J. Loredo, L. E. Kidder, M. A. Scheel, et al. (2013), 1305.5991.
- [32] C. W. Misner, K. S. Thorne, and J. A. Wheeler, *Gravitation* (W. H. Freeman, San Francisco, 1973).
- [33] S. Privitera, S. R. P. Mohapatra, P. Ajith, K. Cannon, N. Fotopoulos, et al. (2013), 1310.5633.
- [34] M. Hannam, P. Schmidt, A. Boh, L. Haegel, S. Husa, et al. (2013), 1308.3271.
- [35] A. Taracchini, Y. Pan, A. Buonanno, E. Barausse, M. Boyle, et al., Phys. Rev. **D86**, 024011 (2012), 1202.0790.
- [36] E. Barausse, V. Morozova, and L. Rezzolla, Astrophys. J. **758**, 63 (2012), 1206.3803.